

Do Wider Neural Networks Really Help Adversarial Robustness?

Boxi Wu^{*†}, Jinghui Chen^{*‡}, Deng Cai[†], Xiaofei He[†], Quanquan Gu[§]

Abstract

Adversarial training is a powerful type of defense against adversarial examples. Previous empirical results suggest that adversarial training requires wider networks for better performances. However, it remains elusive how neural network width affects model robustness. In this paper, we carefully examine the relationship between network width and model robustness. Specifically, we show that the model robustness is closely related to the tradeoff between natural accuracy and perturbation stability, which is controlled by the robust regularization parameter λ . With the same λ , wider networks can achieve better natural accuracy but worse perturbation stability, leading to a potentially worse overall model robustness. To understand the origin of this phenomenon, we further relate the perturbation stability with the network’s local Lipschitzness. By leveraging recent results on neural tangent kernels, we theoretically show that wider networks tend to have worse perturbation stability. Our analyses suggest that: 1) the common strategy of first fine-tuning λ on small networks and then directly use it for wide model training could lead to deteriorated model robustness; 2) one needs to properly enlarge λ to unleash the robustness potential of wider models fully. Finally, we propose a new Width Adjusted Regularization (WAR) method that adaptively enlarges λ on wide models and significantly saves the tuning time.

1 Introduction

Researchers have found that Deep Neural Networks (DNNs) suffer badly from adversarial examples (Szegedy et al., 2014). By perturbing the original inputs with an intentionally computed, undetectable noise, one can deceive DNNs and even arbitrarily modify their predictions on purpose. To defend against adversarial examples and further improve model robustness, various defense approaches have been proposed (Papernot et al., 2016b; Meng and Chen, 2017; Dhillon et al., 2018; Liao et al., 2018; Xie et al., 2018; Guo et al., 2018; Song et al., 2018; Samangouei et al., 2018). Among them, adversarial training Goodfellow et al. (2015); Madry et al. (2018) has been shown to be the most effective type of defenses (Athalye et al., 2018). Adversarial training can be seen as a form of data

^{*}Equal contribution.

[†]State Key Lab of CAD&CG, College of Computer Science, Zhejiang University; E-mail: wuboxi@zju.edu.cn; {dengcai,xiaofeihe}@cad.zju.edu.cn.

[‡]College of Information Science and Technology, Pennsylvania State University, State College, PA 16802, USA; E-mail: jzc5917@psu.edu.

[§]Department of Computer Science, University of California, Los Angeles, CA 90095, USA; E-mail: qgu@cs.ucla.edu.

augmentation by first finding the adversarial examples and then training DNN models on those examples. Specifically, given a DNN classifier f parameterized by θ , a general form of adversarial training with loss function \mathcal{L} can be defined as:

$$\operatorname{argmin}_{\theta} \frac{1}{N} \sum_{i=1}^N \left[\underbrace{\mathcal{L}(\theta; \mathbf{x}_i, y_i)}_{\text{natural risk}} + \lambda \cdot \underbrace{\max_{\hat{\mathbf{x}}_i \in \mathbb{B}(\mathbf{x}_i, \epsilon)} [\mathcal{L}(\theta; \hat{\mathbf{x}}_i, y_i) - \mathcal{L}(\theta; \mathbf{x}_i, y_i)]}_{\text{robust regularization}} \right], \quad (1.1)$$

where $\{(\mathbf{x}_i, y_i)_{i=1}^n\}$ are training data, $\mathbb{B}(\mathbf{x}, \epsilon) = \{\hat{\mathbf{x}} \mid \|\hat{\mathbf{x}} - \mathbf{x}\|_p \leq \epsilon\}$ denotes the ℓ_p norm ball with radius ϵ centered at \mathbf{x} , and $p \geq 1$, and $\lambda > 0$ is the regularization parameter. Compared with standard empirical risk minimization, the extra robust regularization term encourages the data points within $\mathbb{B}(\mathbf{x}, \epsilon)$ to be classified as the same class, i.e., encourages the predictions to be stable. The regularization parameter λ adjusts the strength of robust regularization. When $\lambda = 1$, it recovers the formulation in Madry et al. (2018), and when $\lambda = 0.5$, it recovers the formulation in Goodfellow et al. (2015). Furthermore, replacing the loss difference in robust regularization term with the KL-divergence based regularization recovers the formulation in Zhang et al. (2019).

One common belief in the practice of adversarial training is that, compared with the standard empirical risk minimization, adversarial training requires much wider neural networks to achieve better robustness. Madry et al. (2018) provided an intuitive explanation: robust classification requires a much more complicated decision boundary, as it needs to handle the presence of possible adversarial examples. However, it remains elusive how the network width affects model robustness. To answer this question, we first examine whether the larger network width contributes to both the natural risk term and the robust regularization term in (1.1). Interestingly, when tracing the value changes in (1.1) during adversarial training, we observe that the value of the robust regularization part actually gets worse on wider models, suggesting that larger network width does not lead to better stability in predictions. In Figure 1, we show the loss value comparison of two different wide models trained by TRADES (Zhang et al., 2019) with $\lambda = 6$ as suggested in the original paper. We can see that the wider model (i.e., WideResNet-34-10) achieves better natural risk but incurs a larger value on robust regularization. This motivates us to find out the cause of this phenomenon.

In this paper, we study the relationship between neural network width and model robustness for adversarially trained neural networks. Our contributions can be summarized as follows:

1. We show that the model robustness is closely related to both natural accuracy and perturbation stability, a new metric we proposed to characterize the strength of robust regularization. The balance between the two is controlled by the robust regularization parameter λ . With the same

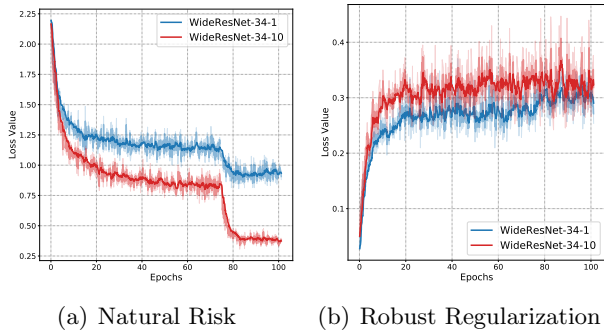


Figure 1: Plots of both natural risk and robust regularization in (1.1). Two 34-layer WideResNet (Zagoruyko and Komodakis, 2016) are trained by TRADES (Zhang et al., 2019) on CIFAR10 (Krizhevsky et al., 2009) with widen factor being 1 and 10.

value of λ , the natural accuracy is improved on wider models while the perturbation stability often worsens, leading to a possible decrease in the overall model robustness. This suggests that proper tuning of λ on wide models is necessary despite being extremely time-consuming, while directly using the fine-tuned λ on small networks to train wider ones, as many people did in practice (Madry et al., 2018; Zhang et al., 2019), may lead to deteriorated model robustness.

2. Unlike previous understandings that there exists a trade-off between natural accuracy and robust accuracy, we show that the real trade-off should be between natural accuracy and perturbation stability. And the robust accuracy is actually the consequence of this trade-off.
3. To understand the origin of the lower perturbation stability of wider networks, we further relate perturbation stability with the network’s local Lipschitzness. By leveraging recent results on neural tangent kernels (Jacot et al., 2018; Allen-Zhu et al., 2019; Zou et al., 2020; Cao and Gu, 2019; Gao et al., 2019), we show that with the same value of λ , larger network width naturally leads to worse perturbation stability, which explains our empirical findings.
4. Our analyses suggest that to unleash the potential of wider model architectures fully, one should mitigate the perturbation stability deterioration and enlarge robust regularization parameter λ for training wider models. Empirical results verified the effectiveness of this strategy on benchmark datasets. In order to alleviate the heavy burden for tuning λ on wide models, we develop the Width Adjusted Regularization (WAR) method to transfer the knowledge we gain from fine-tuning smaller networks into the training of wider networks and significantly save the tuning time.

Notation. For a d -dimensional vector $\mathbf{x} = [x_1, \dots, x_d]^\top$, we use $\|\mathbf{x}\|_p = (\sum_{i=1}^d |x_i|^p)^{1/p}$ with $p \geq 1$ to denote its ℓ_p norm. $\mathbb{1}(\cdot)$ represents the indicator function and \forall represents the universal quantifier.

2 Related Work

Adversarial attacks: Adversarial examples were first found in Szegedy et al. (2014). Since then, tremendous work have been done exploring the origins of this intriguing property of deep learning (Gu and Rigazio, 2015; Kurakin et al., 2017; Fawzi et al., 2018; Tramèr et al., 2017; Gilmer et al., 2018; Zhang et al., 2020b) as well as designing more powerful attacks (Goodfellow et al., 2015; Papernot et al., 2016a; Moosavi-Dezfooli et al., 2016; Madry et al., 2018; Carlini and Wagner, 2017; Chen and Gu, 2020) under various attack settings. Athalye et al. (2018) identified the gradient masking problem and showed that many defense methods could be broken with a few changes on the attacker. Chen et al. (2017) proposed gradient-free black-box attacks and Ilyas et al. (2018, 2019a); Chen et al. (2020) further improved its efficiency. Recently, Ilyas et al. (2019b); Jacobsen et al. (2019) pointed out that adversarial examples are generated from the non-robust or invariant features hidden in the training data.

Defensive adversarial learning: Many defense approaches have been proposed to directly learn a robust model that can defend against adversarial attacks. Madry et al. (2018) proposed a general framework of robust training by solving a min-max optimization problem. Wang et al. (2019) proposed a new criterion to evaluate the convergence quality quantitatively. Zhang et al. (2019)

theoretically studied the trade-off between natural accuracy and robust accuracy for adversarially trained models. Wang et al. (2020) followed this framework and further improved its robustness by differentiating correctly classified and misclassified examples. Cissé et al. (2017) solve the problem by restricting the variation of outputs with respect to the inputs. Cohen et al. (2019); Salman et al. (2019); Lécuyer et al. (2019) developed provably robust adversarial learning methods that have the theoretical guarantees on robustness. Recent works in Wong et al. (2020); Qin et al. (2019) focus on creating adversarial robust networks with faster training protocol. Another line of works focuses on increasing the effective size of the training data, either by pre-trained models Hendrycks et al. (2019) or by semi-supervised learning Carmon et al. (2019); Alayrac et al. (2019); Najafi et al. (2019). Very recently, Wu et al. (2020) proposed to conduct adversarial weight perturbation aside from input perturbation to obtain more robust models. Goyal et al. (2020) achieves further robust models by practical techniques like weight averaging.

Robustness and generalization: Earlier works like Goodfellow et al. (2015) found that adversarial learning can reduce overfitting and help generalization. However, as the arms race between attackers and defenses keeps going, it is observed that strong adversarial attacks can cause severe damage to the model’s natural accuracy Madry et al. (2018); Zhang et al. (2019). Many works (Zhang et al., 2019; Tsipras et al., 2019; Raghunathan et al., 2019; Dobriban et al., 2020) attempt to explain this trade-off between robustness and natural generalization, while some other works proposed different perspectives. Schmidt et al. (2018) confirmed that more training data has the potential to close this gap. Bubeck et al. (2019) suggested that a robust model is computationally difficult to learn and optimize. Zhang et al. (2020b) showed that there is still a large gap between the currently achieved model robustness and the theoretically achievable robustness limit on natural image distributions. Allen-Zhu and Li (2020) showed that the adversarial examples stems from the accumulation of small dense mixtures in the hidden weights during training and adversarial training works by removing such mixtures. Very recently, Raghunathan et al. (2020) showed that this trade-off stems from overparameterization and insufficient data in the linear regression setting. Yang et al. (2020) proved that both accuracy and robustness are achievable through locally Lipschitz functions with separated data, and the gap between theory and practice is due to either failure to impose local Lipschitzness or insufficient generalization. Bubeck et al. (2020) also studied the relationship between robustness and network size. In particular, Bubeck et al. (2020) shows that overparametrization is necessary for robustness on two-layer neural network, while we show that when networks get wider, they will have worse perturbation stability and therefore larger regularization is needed to achieve better robustness.

3 Empirical Study on Network Width and Adversarial Robustness

In this section, we empirically study the relation between network width and robustness by first taking a closer look at the robust accuracy and the associated robust examples.

3.1 Characterization of Robust Examples

Robust accuracy is the standard evaluation metric of robustness, which measures the ratio of robust examples, i.e., examples that can still be correctly classified after adversarial attacks.

Previous empirical results suggest that wide models enjoy both better generalization ability and model robustness. Specifically, Madry et al. (2018) proposed to extend ResNet (He et al., 2016b) architecture to WideResNet (Zagoruyko and Komodakis, 2016) with a widen factor 10 for adversarial training on the CIFAR10 dataset and found that the increased model capacity significantly improves both robust accuracy and natural accuracy. Later works Zhang et al. (2019); Wang et al. (2020) follow this finding and report their best result using the wide networks.

However, as shown by our findings in Figure 1, wider models actually lead to worse robust regularization effects, suggesting that wider models are not better in all aspects, and the relation between model robustness and network width may be more intricate than what people understood previously. To understand the intrinsic relationship between model robustness and network width, let us first take a closer look at the robust examples. Mathematically, robust examples can be defined as $\mathcal{S}_{\text{rob}} := \{\mathbf{x} : \forall \hat{\mathbf{x}} \in \mathbb{B}(\mathbf{x}, \epsilon), f(\boldsymbol{\theta}; \hat{\mathbf{x}}) = y\}$. Note that by definition of robust examples, we have the following equation holds:

$$\underbrace{\{\mathbf{x} : \forall \hat{\mathbf{x}} \in \mathbb{B}(\mathbf{x}, \epsilon), f(\boldsymbol{\theta}; \hat{\mathbf{x}}) = y\}}_{\text{robust examples: } \mathcal{S}_{\text{rob}}} = \underbrace{\{\mathbf{x} : f(\boldsymbol{\theta}; \mathbf{x}) = y\}}_{\text{correctly classified examples: } \mathcal{S}_{\text{correct}}} \wedge \underbrace{\{\mathbf{x} : \forall \hat{\mathbf{x}} \in \mathbb{B}(\mathbf{x}, \epsilon), f(\boldsymbol{\theta}; \mathbf{x}) = f(\boldsymbol{\theta}; \hat{\mathbf{x}})\}}_{\text{stable examples: } \mathcal{S}_{\text{stable}}}, \quad (3.1)$$

where \wedge is the logical conjunction operator. (3.1) suggests that the robust examples are the intersection of two other sets: the correctly classified examples (examples whose predictions are the correct labels) and the stable examples (examples whose predictions are the same within the ℓ_p norm ball). A more direct illustration of this relationship can be found in Figure 2. While the natural accuracy measures the ratio of correctly classified examples $|\mathcal{S}_{\text{correct}}|$ against the whole sample set, to our knowledge, there does not exist a metric measuring the ratio of stable examples $|\mathcal{S}_{\text{stable}}|$ against whole the sample set. Here we formally define this ratio as the *perturbation stability*, which measures the fraction of examples whose predictions cannot be perturbed as reflected in the robust regularization term in (1.1).

3.2 Evaluation of Perturbation Stability

We apply the TRADES Zhang et al. (2019) method, which is one of the strongest baselines in robust training, on CIFAR10 dataset and plot the robust accuracy, natural accuracy, and perturbation stability against the training epochs in Figure 3. Experiments are conducted on WideResNet-34 (Zagoruyko and Komodakis, 2016) with various widen factors. For each network, when robust accuracy reaches the highest point, we record all three metrics and show their changing trend against network width in Figure 3(d). From Figure 3(d), we can observe that the perturbation

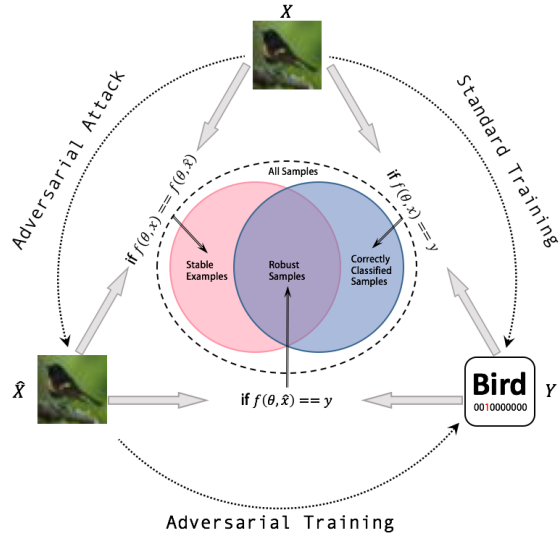


Figure 2: An illustration of robust, correctly classified, and stable examples in (3.1).

stability decreases monotonically as the network width increases. This suggests that wider models are actually more vulnerable to adversarial perturbation. In this sense, the increased network width could hurt the overall model robustness to a certain extent. This can be seen from Figure 3(d), where the robust accuracy of widen-factor 5 is actually slightly better than that of widen-factor 10.

Aside from the relation with model width, we can also gain other insights from perturbation stability:

1. Unlike robust accuracy and natural accuracy, perturbation stability gradually gets worse during the training process. This makes sense since an untrained model that always outputs the same label will have perfect stability, and the training process tends to break this perfect stability. From another perspective, the role of robust regularization in (1.1) is to encourage perturbation stability, such that the model predictions remain the same under small perturbations, which in turn improves model robustness.
2. Previous works (Zhang et al., 2019; Tsipras et al., 2019; Raghunathan et al., 2019) have argued that there exists a trade-off between natural accuracy and robust accuracy. However, from (3.1), we can see that robust accuracy and natural accuracy are coupled with each other, as a robust example must first be correctly classified. When the natural accuracy goes to zero, the robust accuracy will become zero. On the other hand, higher natural accuracy also implies that more examples will likely become robust examples. Works including Raghunathan et al. (2020) and Nakkiran (2019) also challenged this robust-natural trade-off Tsipras et al. (2019) does not hold for some cases. Therefore, we argue that the real trade-off here should be between natural accuracy and perturbation stability and the robust accuracy is actually the consequence of this trade-off.
3. Rice et al. (2020) has recently shown that adversarial training suffers from over-fitting as the robust accuracy might get worse as training proceeds, which can be seen in Figure 3(a). We found that the origin of this over-fitting is mainly attributed to the degenerate perturbation stability (Figure 3(c)) rather than the natural risk (Figure 3(b)). Future works of adversarial training may consider evaluating our perturbation stability to understand how their method takes effects: do they only help natural risk, or robust regularization, or maybe both of them?

4 Why Larger Network Width Leads to Worse Perturbation Stability?

Our empirical findings in Section 3 illustrates how the larger network width may not help model robustness as it leads to worse perturbation stability. However, it still remains unclear what the underlying reasons are for the negative correlation between the perturbation stability and the model width. In this section, we show that larger network width naturally leads to worse perturbation stability from a theoretical perspective. Specifically, we first relate perturbation stability with the network’s local Lipschitzness and then study the relationship between local Lipschitzness and the model width by leveraging recent studies on neural tangent kernels (Jacot et al., 2018; Allen-Zhu et al., 2019; Cao and Gu, 2019; Zou et al., 2020; Gao et al., 2019).

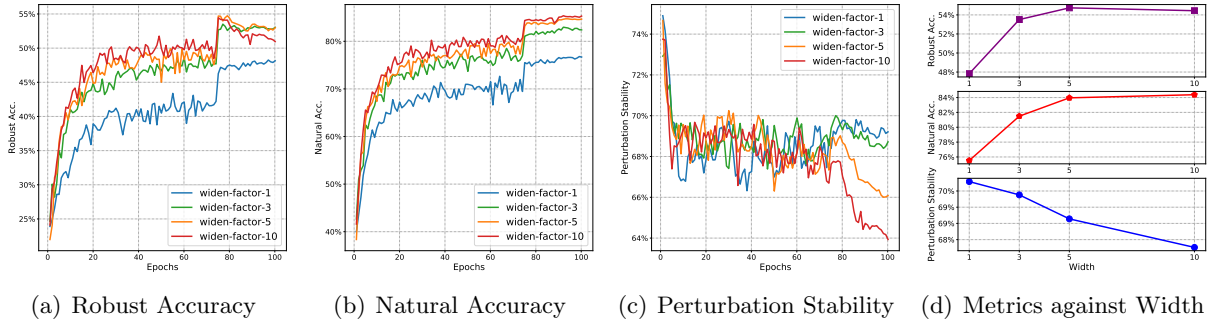


Figure 3: Plots of (a) robust accuracy, (b) natural accuracy, and (c) perturbation stability against training epochs for networks of different width. Results are acquired on CIFAR10 with the adversarial training method TRADES and architectures of WideResNet-34. Training schedule is the same as the original work [Zhang et al. \(2019\)](#). We record all three metrics when robust accuracy reaches the highest point and plot them against network width in (d).

4.1 Perturbation Stability and Local Lipschitzness

Previous works ([Hein and Andriushchenko, 2017](#); [Weng et al., 2018](#)) usually relate local Lipschitzness with network robustness, suggesting that smaller local Lipschitzness leads to robust models. Here we show that local Lipschitzness is more directly linked to perturbation stability, through which it further influences model robustness.

As a start, let us first recall the definition of Lipschitz continuity and its relation with gradient norms.

Lemma 4.1 (Lipschitz continuity and gradient norm ([Paulavičius and Žilinskas, 2006](#))). Let $\mathcal{D} \in \mathbb{R}^d$ denotes a convex compact set, f is a Lipschitz function if for all $\mathbf{x}, \mathbf{x}' \in \mathcal{D}$, it satisfies

$$|f(\mathbf{x}') - f(\mathbf{x})| \leq L \|\mathbf{x}' - \mathbf{x}\|_p,$$

where $L = \sup_{\mathbf{x} \in \mathcal{D}} \{\|\nabla f(\mathbf{x})\|_q\}$ and $1/p + 1/q = 1$.

Intuitively speaking, Lipschitz continuity guarantees that small perturbation in the input will not lead to large changes in the function output. In the adversarial training setting where the perturbation \mathbf{x}' can only be chosen within the neighborhood of \mathbf{x} , we focus on the local Lipschitz constant where we restrict $\mathbf{x}' \in \mathbb{B}(\mathbf{x}, \epsilon)$ and $L = \sup_{\mathbf{x}' \in \mathbb{B}(\mathbf{x}, \epsilon)} \{\|\nabla f(\mathbf{x}')\|_q\}$.

Now suppose our neural network loss function is local Lipschitz, let \mathbf{x}' be our computed adversarial example $\hat{\mathbf{x}}$ and \mathbf{x} be the original example, the robust regularization term satisfies

$$\max_{\hat{\mathbf{x}} \in \mathbb{B}(\mathbf{x}, \epsilon)} [\mathcal{L}(\boldsymbol{\theta}; \hat{\mathbf{x}}, y) - \mathcal{L}(\boldsymbol{\theta}; \mathbf{x}, y)] \leq L \max_{\hat{\mathbf{x}} \in \mathbb{B}(\mathbf{x}, \epsilon)} [\|\hat{\mathbf{x}} - \mathbf{x}\|_p] \leq \epsilon L, \quad (4.1)$$

where the first inequality is due to local Lipschitz continuity and $L = \sup_{\mathbf{x}' \in \mathbb{B}(\mathbf{x}, \epsilon)} \{\|\nabla \mathcal{L}(\boldsymbol{\theta}; \mathbf{x}', y)\|_q\}$. (4.1) shows that the local Lipschitz constant is directly related to the robust regularization term, which can be used as a surrogate loss for the perturbation stability.

4.2 Local Lipschitzness and Network Width

Now we study how the network width affects the perturbation stability via studying the local Lipschitz constant.

Recently, a line of research emerges, which tries to theoretically understand the optimization and generalization behaviors of over-parameterized deep neural networks through the lens of the neural tangent kernel (NTK) (Jacot et al., 2018; Allen-Zhu et al., 2019; Cao and Gu, 2019; Zou et al., 2020). By showing the equivalence between over-parameterized neural networks and NTK in the finite width setting, this type of analysis characterizes the optimization and generalization performance of deep learning by the network architecture (e.g., network width, which we are particularly interested in). Recently, Gao et al. (2019) also analyzed the convergence of adversarial training for over-parameterized neural networks using NTK. Here, we will show that the local Lipschitz constant increases with the model width.

In specific, let m be the network width and H be the network depth. Define an H -layer fully connected neural network as follows

$$f(\mathbf{x}) = \mathbf{a}^\top \sigma(\mathbf{W}^{(H)}) \sigma(\mathbf{W}^{(H-1)}) \dots \sigma(\mathbf{W}^{(1)} \mathbf{x} \dots),$$

where $\mathbf{W}^{(1)} \in \mathbb{R}^{m \times d}$, $\mathbf{W}^{(h)} \in \mathbb{R}^{m \times m}$, $h = 2, \dots, H$ are the weight matrices, $\mathbf{a} \in \mathbb{R}^m$ is the output layer weight vector, and $\sigma(\cdot)$ is the entry-wise ReLU activation function. For notational simplicity, we denote by $\mathbf{W} = \{\mathbf{W}^{(H)}, \dots, \mathbf{W}^{(1)}\}$ the collection of weight matrices and by $\mathbf{W}_0 = \{\mathbf{W}_0^{(H)}, \dots, \mathbf{W}_0^{(1)}\}$ the collection of initial weight matrices. Following Gao et al. (2019), we assume the first layer and the last layer’s weights are fixed, and \mathbf{W} is updated via projected gradient descent with projection set $B(R) = \{\mathbf{W} : \|\mathbf{W}^{(h)} - \mathbf{W}_0^{(h)}\|_F \leq R/\sqrt{m}, h = 1, 2, \dots, H\}$. We have the following lemma upper bounding the input gradient norm.

Lemma 4.2. For any given input $\mathbf{x} \in \mathbb{R}^d$ and ℓ_2 norm perturbation limit ϵ , if $m \geq \max(d, \Omega(H \log(H)))$, $R/\sqrt{m} + \epsilon \leq c/(H^6(\log m)^3)$ for some sufficient small $c > 0$, then with probability at least $1 - O(H)e^{-\Omega(m(R/\sqrt{m} + \epsilon)^{2/3}H)}$, we have for any $\mathbf{x}' \in \mathbb{B}(\mathbf{x}, \epsilon)$ and Lipschitz loss \mathcal{L} , the input gradient norm satisfies

$$\|\nabla \mathcal{L}(f(\mathbf{x}'), y)\|_2 = O(\sqrt{mH}).$$

The proof of Lemma 4.2 can be found in the supplemental materials. Note that Lemma 4.2 holds for any $\mathbf{x}' \in \mathbb{B}(\mathbf{x}, \epsilon)$, therefore, the maximum input gradient norm in the ϵ -ball is also in the order of $O(\sqrt{mH})$. Lemma 4.2 suggests that the local Lipschitz constant is closely related to the neural network width m . In particular, the local Lipschitz constant scales as the square root of the network width. This in theory explains why wider networks are more vulnerable to adversarial perturbation.

In order to further verify the above theoretical result, we empirically calculate the local Lipschitz constant. In detail, for commonly used ℓ_∞ norm threat model, we evaluate the quantity $\sup_{\mathbf{x}' \in \mathbb{B}(\mathbf{x}, \epsilon)} \{\|\nabla \mathcal{L}(\boldsymbol{\theta}; \mathbf{x}', y)\|_1\}$ along the adversarial training trajectory for networks with different widths. Note that solving this maximization problem along the entire training trajectory is computationally expensive or even intractable. Therefore, we approximate this quantity by choosing the maximum input gradient ℓ_1 -norm among the 10 attack steps for each iteration. Figure 4 shows that larger network width indeed leads to larger local Lipschitz constant values. This backup the theoretical results in Lemma 4.2.

5 Experiments

From Section 4, we know that wider networks have worse perturbation stability. This suggests that to fully unleash the potential of wide model architectures, we need to carefully control the decreasing of the perturbation stability on wide models. One natural strategy to do this is by adopting a larger robust regularization parameter λ in (1.1). In this section, we conduct thorough experiments to verify whether this strategy can mitigate the negative effects on perturbation stability and achieve better performances for wider networks.

It is worth noting that due to the high computational overhead of adversarial training on wide networks, previous works (Zhang et al., 2019) tuned λ on smaller networks (ResNet18 He et al. (2016a)) and directly apply it on wider ones, neglecting the influence of model capacity. Our analysis suggests that using the same λ for models with different widths is suboptimal, and one should use a larger λ for wider models in order to get better model robustness.

5.1 Experimental Settings

We conduct our experiments on CIFAR10 (Krizhevsky et al., 2009) dataset, which is the most popular dataset in the adversarial training literature. It contains images from 10 different categories, with $50k$ images for training and $10k$ for testing. Here we first conduct our experiments using the TRADES (Zhang et al., 2019) method. Networks are chosen from WideResNet (Zagoruyko and Komodakis, 2016) with different widen factor from 1, 5, 10. The batch size is set to 128, and we train each model for 100 epochs. The initial learning rate is set to be 0.1. We adopt a slightly different learning rate decay schedule: instead of dividing the learning rate by 10 after 75-th epoch and 90-th epoch as in Madry et al. (2018); Zhang et al. (2019); Wang et al. (2020), we halve the learning rate for every epoch after the 75-th epoch, for the purpose of preventing over-fitting. For evaluating the model robustness, we perform the standard PGD attack (Madry et al., 2018) using 20 steps with step size 0.007, and $\epsilon = 8/255$. Note that previous works (Zhang et al., 2019; Wang et al., 2020) report their results using step size 0.003, which we found is actually less effective than ours. All experiments are conducted on a single NVIDIA V100 GPU.

5.2 Model Robustness with Larger Robust Regularization Parameter

We first compare the robustness performance of models with different network width using robust regularization parameters chosen from $\{6, 9, 12, 15, 18, 21\}$ for TRADES (Zhang et al., 2019). Results of different evaluation metrics are presented in Table 1.

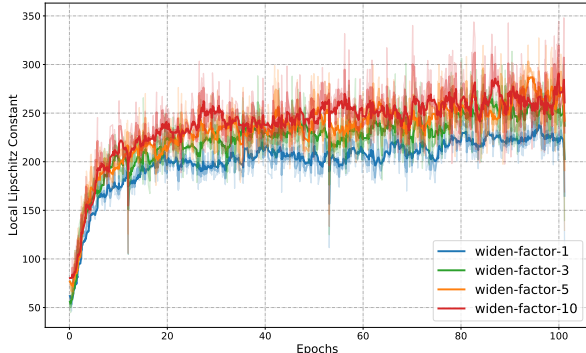


Figure 4: Plot of approximated local Lipschitz constant along the adversarial training trajectory. Models are trained by TRADES (Zhang et al., 2019) on CIFAR10 dataset using WideResNet model. Wider networks in general have larger local Lipschitz constants.

Table 1: The three metrics under PGD attack with different λ on CIFAR10 dataset using WideResNet-34 model. We test TRADES as well as our (generalized) adversarial training. Each experiment is repeated three times. The highest robustness value for each column is annotated with bold number. From the table, we can tell that: 1) The best choice of λ increases as the network width increases; 2) For models with the same width, the larger λ always leads to higher perturbation stability; 3) With the same λ , the larger width always hurts perturbation stability, which backs up our claim in Section 4.2.

λ	Robust Accuracy (%)			Natural Accuracy (%)			Perturbation Stability (%)		
	width-1	width-5	width-10	width-1	width-5	width-10	width-1	width-5	width-10
TRADES Zhang et al. (2019)									
6	47.81±.09	54.45±.16	54.18±.39	76.26±.10	84.44±.06	84.90±.80	69.33±.05	68.27±.22	67.25±.39
9	48.01±.06	55.34±.17	55.29±.45	73.78±.30	82.77±.07	84.13±.28	71.92±.33	70.66±.26	69.08±.80
12	47.87±.06	55.61±.04	55.98±.13	72.29±.25	81.59±.20	83.59±.62	73.33±.16	72.00±.20	70.18±.67
15	47.15±.13	55.49±.15	55.96±.09	70.98±.24	80.69±.08	82.81±.19	73.79±.27	72.87±.03	70.87±.23
18	47.02±.13	55.43±.12	56.43±.17	70.13±.06	79.97±.12	82.21±.21	74.63±.11	73.77±.13	72.04±.30
21	46.26±.19	55.31±.20	56.07±.21	68.95±.38	79.25±.23	81.74±.12	75.17±.28	74.15±.38	72.11±.12
Adversarial Training Madry et al. (2018)									
1.00	47.99±.16	50.87±.42	50.12±.13	77.30±.01	85.82±.01	85.62±.81	66.48±.24	62.23±.42	61.62±.46
1.25	49.24±.12	53.10±.09	51.97±.46	74.04±.47	84.73±.22	86.25±.12	70.34±.54	65.24±.08	62.94±.35
1.50	49.11±.03	54.15±.03	53.25±.52	72.16±.25	84.35±.19	85.50±.57	72.10±.11	66.65±.06	64.51±.72
1.75	48.32±.63	54.36±.14	53.65±.80	70.66±.46	83.95±.30	85.52±.24	72.43±.40	67.31±.03	65.67±.10
2.00	47.44±.06	54.10±.15	55.78±.22	69.67±.09	83.49±.06	85.41±.13	72.73±.04	67.53±.01	65.71±.15

From Table 1, we can observe that the best robust accuracy for width-1 network is achieved when $\lambda = 9$, yet for width-5 network, the best robust accuracy is achieved when $\lambda = 12$, and for width-10 network, the best λ is 18. This suggests that wider networks indeed need a larger robust regularization parameter to unleash the power of wide model architecture fully. Our exploration also suggests that the optimal choice of λ for width-10 network is 18 under the same setting as [Zhang et al. \(2019\)](#), which is three times larger than the one used in the original paper, leading to an average improvement of 2.25% on robust accuracy. It is also worth noting that enlarging λ indeed leads to improved perturbation stability. Under the same λ , wider networks have worse perturbation stability. This observation is rather consistent with our empirical and theoretical findings in Sections 3 and 4. As stated in Section 3.2, the real trade-off is between natural accuracy and perturbation stability rather than robust accuracy. Also, the stability provides a clear hint for finding the best choice of λ .

We further show that our strategy also applies to the original adversarial training [Madry et al. \(2018\)](#), as shown by the bottom part of Table 1. Proper adaptations should be made to boost the robust regularization for original (generalized) adversarial training. We show the detail of the adaptations in the Appendix. As shown by the table, the large improvements on both TRADES and adversarial training using our boosting strategy suggest that adopting larger λ is crucial in unleashing the full potential of wide models, which is usually neglected in practice.

Table 2: Robust accuracy (%) for different datasets, architectures and regularization parameters under various attacks. The highest results are evaluated for three times of randomly started attack. Our approach of boosting regularization for wider models apply to all cases. The value of w and k represents the network width.

Dataset	Architecture	widen-factor/ growth-rate	regulari- zation	PGD	C&W	FAB	Square
CIFAR10	WideResNet-34	$w = 1$	$\lambda = 6$	47.92±.01	44.95±.03	44.31±.04	49.25±.02
			$\lambda = 12$	47.91±.04	44.24±.02	43.71±.05	47.75±.02
			$\lambda = 18$	46.92±.05	43.48±.03	43.00±.01	46.01±.05
		$w = 5$	$\lambda = 6$	54.50±.03	53.14±.03	52.13±.05	56.79±.02
			$\lambda = 12$	55.56±.04	53.28±.04	52.55±.02	56.88±.05
			$\lambda = 18$	55.21±.02	52.64±.02	52.18±.01	56.31±.01
	$w = 10$	$\lambda = 6$	54.23±.04	54.02±.03	52.68±.07	57.64±.03	
		$\lambda = 12$	55.80±.06	54.41±.01	53.57±.04	57.72±.10	
		$\lambda = 18$	56.29±.10	54.57±.02	54.06±.02	58.04±.05	
	DenseNet-BC-40	$k = 12$	$\lambda = 6$	44.79±.02	40.83±.03	40.07±.03	45.66±.05
			$\lambda = 12$	44.66±.03	40.91±.03	39.88±.01	44.23±.04
			$\lambda = 18$	44.38±.05	40.63±.03	39.42±.01	43.31±.04
$k = 64$		$\lambda = 6$	55.51±.01	52.76±.04	51.74±.02	57.24±.01	
		$\lambda = 12$	55.85±.03	52.98±.02	52.10±.03	57.34±.04	
		$\lambda = 18$	55.71±.03	52.83±.06	51.66±.04	55.21±.03	
CIFAR100	WideResNet-34	$w = 1$	$\lambda = 6$	24.28±.02	20.24±.01	19.97±.02	22.91±.02
			$\lambda = 12$	24.18±.04	20.15±.02	19.83±.01	22.78±.01
			$\lambda = 18$	23.99±.03	20.01±.02	19.01±.01	22.04±.01
		$w = 5$	$\lambda = 6$	30.73±.03	27.25±.05	26.01±.03	30.11±.03
			$\lambda = 12$	31.57±.02	27.83±.02	27.08±.01	30.45±.01
			$\lambda = 18$	31.38±.01	27.66±.04	26.94±.03	30.02±.01
	$w = 10$	$\lambda = 6$	30.48±.02	27.98±.01	27.00±.11	30.45±.06	
		$\lambda = 12$	31.75±.09	29.25±.04	28.14±.03	31.23±.04	
		$\lambda = 18$	32.98±.03	29.83±.01	28.78±.02	32.02±.01	

5.3 Experiments on Different Datasets and Architectures

To show that our theory is universal and is applicable to various datasets and architectures, we conduct extra experiments on the CIFAR100 dataset and DenseNet model [Huang et al. \(2017\)](#). For the DenseNet models, the growth rate k denotes how fast the number of channels grows and thus becomes a suitable measure of network width. Following the original paper [Huang et al. \(2017\)](#), we choose DenseNet-BC-40 and use models with different growth rates to verify our theory.

Experimental results are shown in Table 2. For completeness, we also report the results under four different attack methods and settings, including PGD [Madry et al. \(2018\)](#), C&W [Carlini and Wagner \(2017\)](#), FAB [Croce and Hein \(2020a\)](#), and Square [Andriushchenko et al. \(2020\)](#). We adopt the best λ from Table 1 and show the corresponding performance on models with different widths. It can be seen that our strategy of using a larger robust regularization parameter works very well across different datasets and networks. On the WideResNet model, we observe clear patterns as in

Section 5.2. On the DenseNet model, although the best regularization λ is different from that of WideResNet, wider models, in general, still require larger λ for better robustness. On CIFAR100, our strategy raises the standard PGD score of the widest model from 30.48% to 32.98%.

5.4 Width Adjusted Regularization

Our previous analysis has shown that larger model width may hurt adversarial robustness without properly choosing the regularization parameter λ . However, exhaustively cross-validating λ on wider networks can be extremely time-consuming in practice. To address this issue, we investigate the possibility of automatically adjusting λ according to the model width, based on our existing knowledge obtained in fine-tuning smaller networks, which is much cheaper. Note that the key to achieving the best robustness is to well balance between the natural risk term and the robust regularization term in (1.1). Although the regularization parameter λ cannot be directly applied from thinner networks to wider networks (as suggested by our analyses), the best ratio between the natural risk and the robust regularization across different width models can be kept roughly the same. Following this idea, we design the **Width Adjusted Regularization (WAR)** method, which is summarized in Algorithm 1. Specifically, we first manually tune the best λ for a thin network and record the ratio ζ between the natural risk and the robust regularization when the training converges. Then, on training wider networks, we adaptively¹ adjust λ to encourage the ratio between the natural risk and the robust regularization to stay close to ζ . Let’s take an example here. We first cross-validate λ on a thin network with widen factor 0.5 and identify the best $\lambda = 6$ and $\zeta = 30$ with 18 GPU hours in total. Now we compare three different strategies for training wider models and summarize the results in Table 3: 1) directly apply $\lambda = 6$ with no fine-tuning on the current model; 2) exhaustive manual fine-tuning from $\lambda = 6.0$ to $\lambda = 21.0$ (6 trials) as in Table 1; 3) our WAR strategy. Table 3 shows that the final λ generated by WAR on wider models are consistent with the exhaustively tuned best λ . Compared to the exhaustive manual tuning strategy, WAR achieves even slightly better model robustness with much less overall training time (~ 4 times speedup for WRN-34-10 model). On the other hand, directly using $\lambda = 6$ with no tuning on the wide models leads to much worse model robustness while having the same overall training time. This verifies the effectiveness of our proposed WAR method.

5.5 Comparison of Robustness on Wide Models

Previous experiments in Section 5.2 and Section 5.3 have shown the effectiveness of our proposed strategy on using larger robust regularization parameter for wider models. In order to ensure that this strategy does not lead to any obfuscated gradient problem (Athalye et al., 2018) and gives a false sense of robustness, we further conduct experiments using stronger attacks. In particular, we choose to evaluate our best models on the AutoAttack algorithm (Croce and Hein, 2020b), which is an ensemble attack method that contains four different white-box and black-box attacks for the best attack performances.

We evaluate models trained with WAR, with or without extra unlabeled data Carmon et al. (2019), and report the robust accuracy in Table 4. Note that the results of other baselines are

¹the learning rate α for λ_t in Algorithm 1 is not sensitive and needs no extra tuning.

Algorithm 1 Width Adjusted Regularization

```
1: Input: initial weights  $\theta_0$ , WAR parameter  $\zeta$ ,  
   learning rate  $\eta$ , adversarial attack  $\mathcal{A}$   
2:  $\lambda_0 = 0, \alpha = 0.1$   
3: for  $t = 1, \dots, T$  do  
4:   Get mini-batch  $\{(\mathbf{x}_1, y_1), \dots, (\mathbf{x}_m, y_m)\}$   
5:   for  $i = 1, \dots, m$  (in parallel) do  
6:      $\hat{\mathbf{x}}_i \leftarrow \mathcal{A}(\mathbf{x}_i)$   
7:      $l_{\text{nat}} \leftarrow \mathcal{L}(\theta_t; \mathbf{x}_i, y_i)$   
8:      $l_{\text{rob}} \leftarrow \mathcal{L}(\theta_t; \hat{\mathbf{x}}_i, y_i) - \mathcal{L}(\theta_t; \mathbf{x}_i, y_i)$   
9:      $\lambda_t \leftarrow \max(\lambda_{t-1} + \alpha \cdot (\zeta - (l_{\text{nat}}/l_{\text{rob}})), 0)$   
10:     $\theta_t \leftarrow \theta_{t-1} - (\eta/m) \sum_{i=1}^m \nabla_{\theta} [l_{\text{nat}} + \lambda_t \cdot l_{\text{rob}}]$   
11:   end for  
12: end for
```

Table 3: Comparison of TRADES with different tuning strategies. N/A denotes no fine-tuning of the current model (tuning on small networks only). Manual represents exhaustive fine-tuning.

Model	Tuning	λ	PGD	GPU hours
WRN-34-1	N/A	6.00	47.81	12+18=30
	Manual	9.00	48.01	12×6=72
	WAR	9.12	48.06	12+18=30
WRN-34-5	N/A	6.00	54.45	20+18=38
	Manual	12.00	55.61	20×6=120
	WAR	14.37	55.62	20+18=38
WRN-34-10	N/A	6.00	54.18	32+18=50
	Manual	18.00	56.43	32×6=192
	WAR	16.43	56.46	32+18=50

directly obtained from the AutoAttack leaderboard². From Table 4, we can see that our WAR significantly improves the baseline TRADES models on WideResNet. This experiment further verifies the effectiveness of our proposed strategy.

6 Conclusions

In this paper, we studied the relation between network width and adversarial robustness in adversarial training, a principled approach to train robust neural networks. We showed that the model robustness is closely related to both natural accuracy and perturbation stability, while the balance between the two is controlled by the robust regularization parameter λ . With the same value of λ , the natural accuracy is better on wider models while the perturbation stability actually becomes worse, leading to a possible decrease in the overall model robustness. We showed the origin of this problem by relating perturbation stability with local Lipschitzness and leveraging recent studies

on the neural tangent kernel to prove that larger network width leads to worse perturbation stability. Our analyses suggest that: 1) proper tuning of λ on wider models is necessary despite being extremely time-consuming; 2) practitioners should adopt a larger λ for training wider networks. Finally, we propose the Width Adjusted Regularization, which significantly saves the tuning time for robust training on wide models.

Table 4: Robust accuracy (%) comparison on CIFAR10 under AutoAttack. † indicates training with extra unlabeled data.

Methods	Model	AutoAttack
TRADES Zhang et al. (2019)	WRN-34-10	53.08
Early-Stop Rice et al. (2020)	WRN-34-20	53.42
FAT Zhang et al. (2020a)	WRN-34-10	53.51
HE Pang et al. (2020)	WRN-34-20	53.74
WAR	WRN-34-10	54.73
<hr/>		
MART Wang et al. (2020)†	WRN-28-10	56.29
HYDRA Sehwag et al. (2020)†	WRN-28-10	57.14
RST Carmon et al. (2019)†	WRN-28-10	59.53
WAR†	WRN-28-10	60.02
WAR†	WRN-28-20	61.84

²<https://github.com/fra31/auto-attack>

A Proof of Lemma 4.2

Lemma A.1 (Restatement of Lemma 4.2). For any given input $\mathbf{x} \in \mathbb{R}^d$ and ℓ_2 norm perturbation limit ϵ , if $m \geq \max(d, \Omega(H \log(H)))$, $\frac{R}{\sqrt{m}} + \epsilon \leq \frac{c}{H^6(\log m)^3}$ for some sufficient small c , then with probability at least $1 - O(H)e^{-\Omega(m(R/\sqrt{m} + \epsilon)^{2/3}H)}$, we have for any $\mathbf{x}' \in \mathbb{B}(\mathbf{x}, \epsilon)$ and Lipschitz loss \mathcal{L} , the input gradient norm satisfies

$$\|\nabla \mathcal{L}(f(\mathbf{x}'), y)\|_2 = O(\sqrt{mH}).$$

Proof. The major part of this proof is inspired from Gao et al. (2019). Let $\mathbf{D}^{(h)}(\mathbf{W}, \mathbf{x}) = \text{diag}(\mathbb{1}\{\mathbf{W}^{(h)}\sigma(\dots\sigma(\mathbf{W}^{(1)}\mathbf{x})) > 0\})$ be a diagonal sign matrix. Then the neural network function can be rewritten as follows:

$$f(\mathbf{x}) = \mathbf{a}^\top \mathbf{D}^{(H)}(\mathbf{W}, \mathbf{x}) \mathbf{W}^{(H)} \dots \mathbf{D}^{(1)}(\mathbf{W}, \mathbf{x}) \mathbf{W}^{(1)} \mathbf{x}.$$

By the chain rule of the derivatives, the input gradient norm can be further written as

$$\begin{aligned} \|\nabla \mathcal{L}(f(\mathbf{x}'), y)\|_2 &= \|\mathcal{L}'(f(\mathbf{x}'), y) \cdot \nabla f(\mathbf{x}')\|_2 \\ &\leq \|\mathcal{L}'(f(\mathbf{x}'), y)\|_2 \cdot \|\nabla f(\mathbf{x}')\|_2 \\ &= \|\mathcal{L}'(f(\mathbf{x}'), y)\|_2 \cdot \|\mathbf{a}^\top \mathbf{D}^{(H)}(\mathbf{W}, \mathbf{x}') \mathbf{W}^{(H)} \dots \mathbf{D}^{(1)}(\mathbf{W}, \mathbf{x}') \mathbf{W}^{(1)}\|_2. \end{aligned} \quad (\text{A.1})$$

Now let us focus on the term $\|\mathbf{a}^\top \mathbf{D}^{(H)}(\mathbf{W}, \mathbf{x}') \mathbf{W}^{(H)} \dots \mathbf{D}^{(1)}(\mathbf{W}, \mathbf{x}') \mathbf{W}^{(1)}\|_2$. Note that by triangle inequality,

$$\begin{aligned} &\|\mathbf{a}^\top \mathbf{D}^{(H)}(\mathbf{W}, \mathbf{x}') \mathbf{W}^{(H)} \dots \mathbf{D}^{(1)}(\mathbf{W}, \mathbf{x}') \mathbf{W}^{(1)}\|_2 \\ &\leq \|\mathbf{a}^\top \mathbf{D}^{(H)}(\mathbf{W}, \mathbf{x}') \mathbf{W}^{(H)} \dots \mathbf{D}^{(1)}(\mathbf{W}, \mathbf{x}') \mathbf{W}^{(1)} - \mathbf{a}^\top \mathbf{D}^{(H)}(\mathbf{W}_0, \mathbf{x}) \mathbf{W}_0^{(H)} \dots \mathbf{D}^{(1)}(\mathbf{W}_0, \mathbf{x}) \mathbf{W}_0^{(1)}\|_2 \\ &\quad + \|\mathbf{a}^\top \mathbf{D}^{(H)}(\mathbf{W}_0, \mathbf{x}) \mathbf{W}_0^{(H)} \dots \mathbf{D}^{(1)}(\mathbf{W}_0, \mathbf{x}) \mathbf{W}_0^{(1)}\|_2. \end{aligned} \quad (\text{A.2})$$

Note that \mathbf{W} is updated via projected gradient descent with projection set $B(R)$. Therefore, by Equation (12) in Lemma A.5 of Gao et al. (2019) we have

$$\begin{aligned} &\|\mathbf{a}^\top \mathbf{D}^{(H)}(\mathbf{W}, \mathbf{x}') \mathbf{W}^{(H)} \dots \mathbf{D}^{(1)}(\mathbf{W}, \mathbf{x}') \mathbf{W}^{(1)} - \mathbf{a}^\top \mathbf{D}^{(H)}(\mathbf{W}_0, \mathbf{x}) \mathbf{W}_0^{(H)} \dots \mathbf{D}^{(1)}(\mathbf{W}_0, \mathbf{x}) \mathbf{W}_0^{(1)}\|_2 \\ &= O\left(\left(\frac{R}{\sqrt{m}} + \epsilon\right)^{1/3} H^2 \sqrt{m \log m}\right), \end{aligned} \quad (\text{A.3})$$

and by Lemma A.3 in Gao et al. (2019) we have

$$\|\mathbf{a}^\top \mathbf{D}^{(H)}(\mathbf{W}_0, \mathbf{x}) \mathbf{W}_0^{(H)} \dots \mathbf{D}^{(1)}(\mathbf{W}_0, \mathbf{x}) \mathbf{W}_0^{(1)}\|_2 = O(\sqrt{mH}). \quad (\text{A.4})$$

Combining (A.2), (A.3), (A.4), when $\frac{R}{\sqrt{m}} + \epsilon \leq \frac{c}{H^6(\log m)^3}$, we have

$$\|\mathbf{a}^\top \mathbf{D}^{(H)}(\mathbf{W}, \mathbf{x}') \mathbf{W}^{(H)} \dots \mathbf{D}^{(1)}(\mathbf{W}, \mathbf{x}') \mathbf{W}^{(1)}\|_2 = O(\sqrt{mH}). \quad (\text{A.5})$$

By substituting (A.5) into (A.1) we have,

$$\|\nabla \mathcal{L}(f(\mathbf{x}'), y)\|_2 \leq \|\mathcal{L}'(f(\mathbf{x}'), y)\|_2 \cdot \|\mathbf{a}^\top \mathbf{D}^{(H)}(\mathbf{W}, \mathbf{x}') \mathbf{W}^{(H)} \dots \mathbf{D}^{(1)}(\mathbf{W}, \mathbf{x}') \mathbf{W}^{(1)}\|_2 = O(\sqrt{mH}),$$

where the last inequality holds since $\|\mathcal{L}'(f(\mathbf{x}'), y)\|_2 = O(1)$ due to the Lipschitz condition of loss \mathcal{L} . This concludes the proof. \square

B The Experimental Detail for Reproducibility

All experiments are conducted on a single NVIDIA V100. It runs on the GNU Linux Debian 4.9 operating system. The experiment is implemented via PyTorch 1.6.0. We adopt the public released codes of PGD [Madry et al. \(2018\)](#), TRADES [Zhang et al. \(2019\)](#), and RST [Carmon et al. \(2019\)](#) and adapt them for our own settings, including inspecting the loss value of robust regularization and the local Lipschitzness.

CIFAR100 contains 50k images for 100 classes, which means that it has much fewer images for each class compared with CIFAR10. This makes the learning problem of CIFAR100 much harder. For DenseNet architecture, we adopt the 40 layers model with the bottleneck design, which is the DenseNet-BC-40. It has three building blocks, with each one having the same number of layers. This is the same architecture tested in the original paper of DenseNet for CIFAR10. For simplicity reason, we make the training schedule stay the same with the one used for WideResNet, which is the decay learning rate schedule. As DenseNet gets deeper, its channel number (width) will be multiplied with the growing rate k . Thus, as k gets larger, the width of DenseNet also does. Although this mechanism slightly differs from the widen factor of WideResNet, which amplify all layers with the same ratio.

C The Exponential Decay Learning Rate

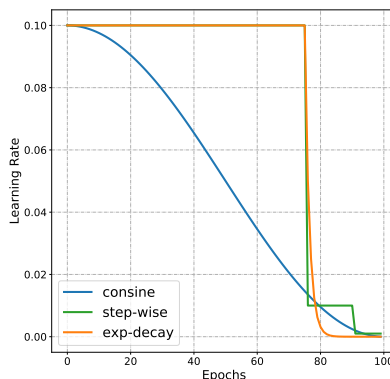


Figure 5: The changing trend learning rate against training epochs for different learning rate schedule.

To demonstrate the fact that the over-fitting problem all comes from perturbation stability in Section 3.2(3), we use the training schedule of the original work for Figure 2. Aside from that, all the other experiments and plots are results under our proposed learning rate schedule, which halve the learning rate for every epochs after the 75-th epoch and can prevent over-fitting. Different learning rate schedules are shown in Figure 5, including the step-wise [Zhang et al. \(2019\)](#), cosine [Carmon et al. \(2019\)](#), and our exp-decay learning rate schedule. Basically, our schedule is an early-stop version of the baseline of TRADES [Zhang et al. \(2019\)](#), which skips the small learning rate stage as soon as possible in the later stage. We found this schedule is the most effective one when only

training on the original CIFAR10. However, when combined with the 500K unlabeled images from RST [Carmon et al. \(2019\)](#), we find that the over-fitting problem is much less severe and cosine learning rate is the best choice.

D Boosting the Original Adversarial Training

We further show that our strategy also applies to the original adversarial training [Madry et al. \(2018\)](#). Note that our generalized adversarial training framework (1.1) allow us to further boost the robust regularization for original (generalized) adversarial training. The only caveat is that in adversarial training formulation, the robust regularization term is not guaranteed to be non-negative in practice³. To avoid this problem, we manually set the robust regularization term in (1.1) to be non-negative by clipping the $\mathcal{L}(\boldsymbol{\theta}; \hat{\mathbf{x}}, y) - \mathcal{L}(\boldsymbol{\theta}; \mathbf{x}, y)$ term. Let us denote \mathbf{x}' as the empirical maximization solution, the final loss function becomes:

$$\operatorname{argmin}_{\boldsymbol{\theta}} \mathbb{E}_{(\mathbf{x}, y) \sim \mathcal{D}} \left\{ \mathcal{L}(\boldsymbol{\theta}; \mathbf{x}, y) + \lambda \cdot \max_{\hat{\mathbf{x}}_i \in \mathbb{B}(\mathbf{x}_i, \epsilon)} (\mathcal{L}(\boldsymbol{\theta}; \mathbf{x}', y) - \mathcal{L}(\boldsymbol{\theta}; \mathbf{x}, y), 0) \right\}.$$

The bottom part of Table 1 shows the experimental results for boosting the robust regularization parameter for (generalized) adversarial training models. We can observe that the boosting strategy still works in this method, and wider models indeed require larger λ to obtain the best robust accuracy.

E Verifying Our Findings on ImageNet

We further test the model of Fast AT [Wong et al. \(2020\)](#) on ImageNet dataset in Table 5, and it again verifies our conclusion that larger model width would increase natural accuracy but decrease perturbation stability.

Table 5: Fast Adversarial Training on ImageNet.

Models	λ	Robust Accuracy	Top5-Natural Accuracy	Perturbation Stability
WideResNet-50-1	1.0	38.34	53.24	72.29
WideResNet-50-2	1.0	51.65	66.67	70.10

F Boosting the Regularization Parameter on Extra Adversarial Training Methods

We also compare with other models from the AutoAttack [Croce and Hein \(2020b\)](#) leaderboard. We focus on the AWP [Wu et al. \(2020\)](#) and show the result in Table 6. We found that our conclusion

³Successfully solving the inner maximization problem in (1.1) is supposed to guarantee that $\mathcal{L}(\boldsymbol{\theta}; \mathbf{x}', y) > \mathcal{L}(\boldsymbol{\theta}; \mathbf{x}, y)$, however, in practice, there still exist a very little chance that $\mathcal{L}(\boldsymbol{\theta}; \mathbf{x}', y) < \mathcal{L}(\boldsymbol{\theta}; \mathbf{x}, y)$ due to failure in solving the inner maximization problem at the beginning of the training procedure with limited steps.

still holds for the AWP method that using larger λ (12.0 rather than 6.0 in the default setting) can achieve even better robust accuracy.

Table 6: AWP on CIFAR10 dataset.

Models	λ	Robust Accuracy	Natural Accuracy	Perturbation Stability
WideResNet-34-10	6.0	59.01	84.82	73.95
WideResNet-34-10	12.0	59.34	81.20	76.65
WideResNet-34-10	18.0	58.72	78.43	77.54

G Evaluating the Three Metrics on State-of-the-Art Models

In the figure below, we evaluate nine state-of-the-art robust models against the PGD attack for the three metrics: the natural accuracy, the perturbation stability, and the robust accuracy (the size of the ball). Our dissection of these three metrics helps the researcher better understand how different approaches influence adversarial robustness. For instance, we can tell that HE [Pang et al. \(2020\)](#) mainly helps the stability, Pretrain [Hendrycks et al. \(2019\)](#) mainly helps the natural accuracy and slightly hurts stability. Moreover, we can tell that methods like RST [Carmon et al. \(2019\)](#) simultaneously improve the natural accuracy and perturbation stability. This observation shows that it is possible to improve the two contradictory metrics.

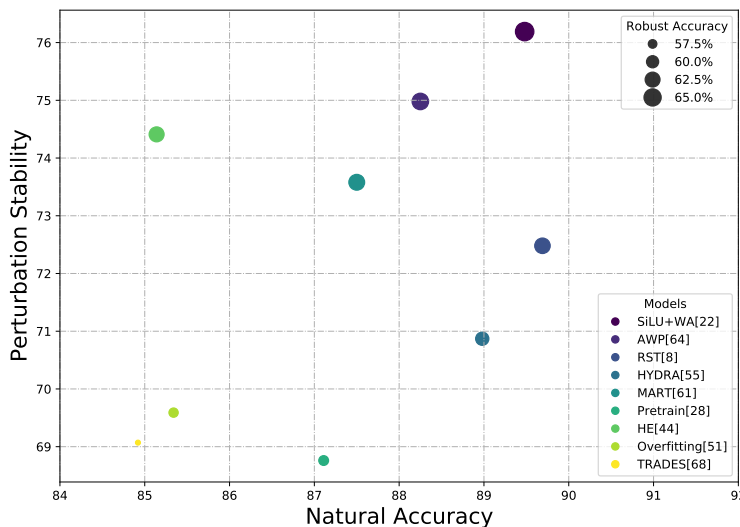


Figure 6: The changing trend learning rate against training epochs for different learning rate schedule.

H More Illustrations of Eqn. (1.1)

In this part, we provide a complete visualization for the two parts in Eqn. (1.1). The figures below are an extension of Figure 1, where the models are those we trained in Table 2. We test WideResNet-34 on CIFAR10 and CIFAR10. We test DenseNet-BC-40 on CIFAR10. The two losses with respect to different robust regularization parameter λ are shown. Again, we emphasize that the observation that wider neural networks achieve worse performance on stability with the same λ can be found during the training stage. Therefore, this intriguing phenomenon is not an over-fitting problem, as previous works Rice et al. (2020) pointed out.

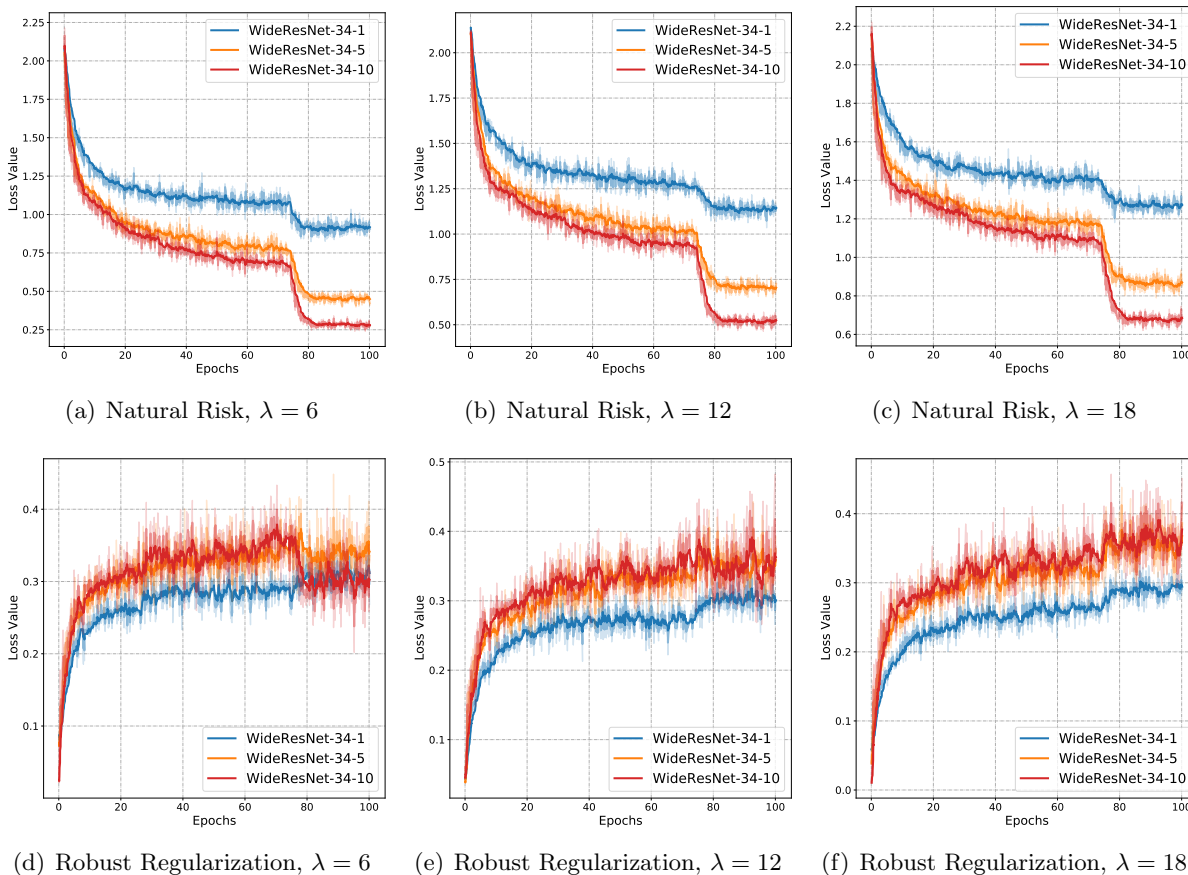


Figure 7: WideResNet-34 on CIFAR10.

References

ALAYRAC, J., UESATO, J., HUANG, P., FAWZI, A., STANFORTH, R. and KOHLI, P. (2019). Are labels required for improving adversarial robustness? In *NeurIPS*.

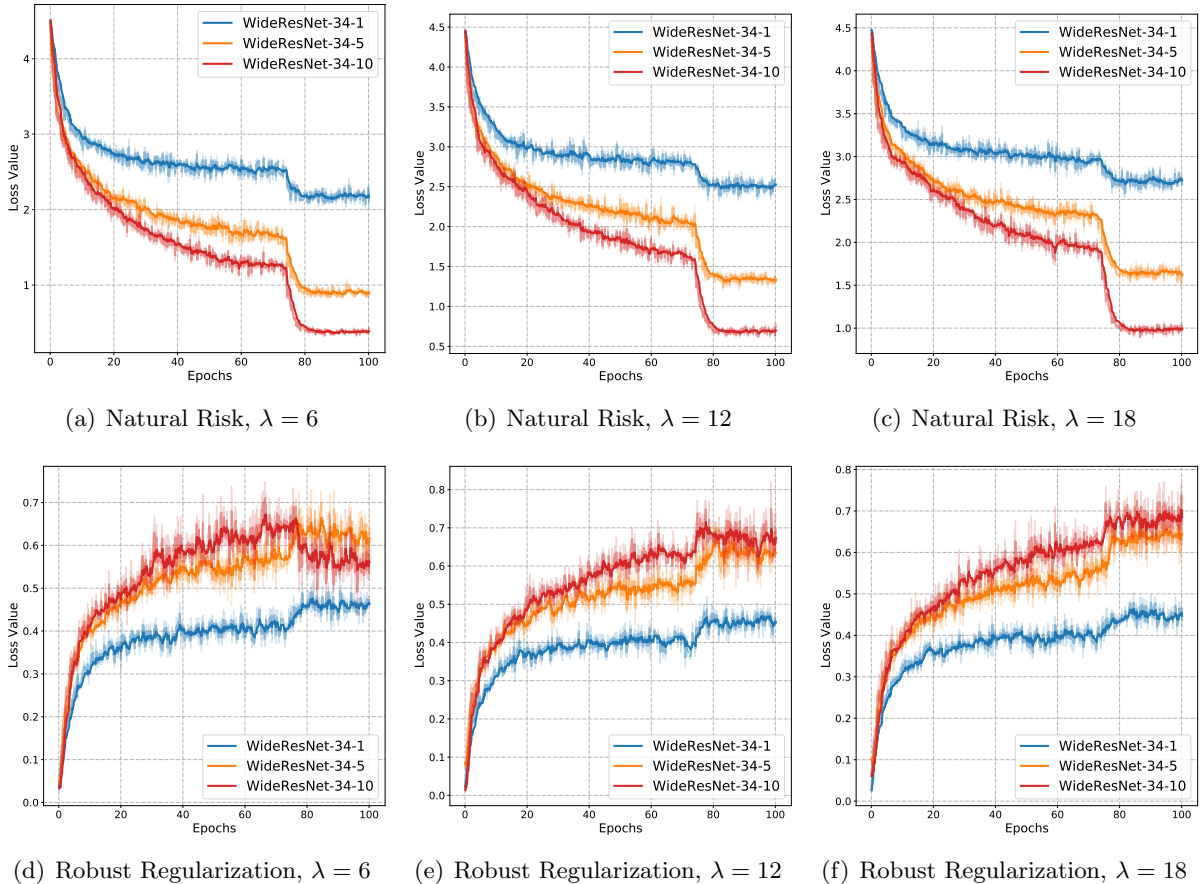


Figure 8: WideResNet-34 on CIFAR100.

ALLEN-ZHU, Z. and LI, Y. (2020). Feature purification: How adversarial training performs robust deep learning. *arXiv preprint arXiv:2005.10190* .

ALLEN-ZHU, Z., LI, Y. and SONG, Z. (2019). A convergence theory for deep learning via over-parameterization. In *International Conference on Machine Learning*. PMLR.

ANDRIUSHCHENKO, M., CROCE, F., FLAMMARION, N. and HEIN, M. (2020). Square attack: A query-efficient black-box adversarial attack via random search. In *ECCV* (A. Vedaldi, H. Bischof, T. Brox and J. Frahm, eds.), vol. 12368 of *Lecture Notes in Computer Science*. Springer.

ATHALYE, A., CARLINI, N. and WAGNER, D. A. (2018). Obfuscated gradients give a false sense of security: Circumventing defenses to adversarial examples. In *ICML*, vol. 80 of *Proceedings of Machine Learning Research*. PMLR.

BUBECK, S., LEE, Y. T., PRICE, E. and RAZENSHTEYN, I. P. (2019). Adversarial examples from computational constraints. In *ICML*, vol. 97 of *Proceedings of Machine Learning Research*. PMLR.

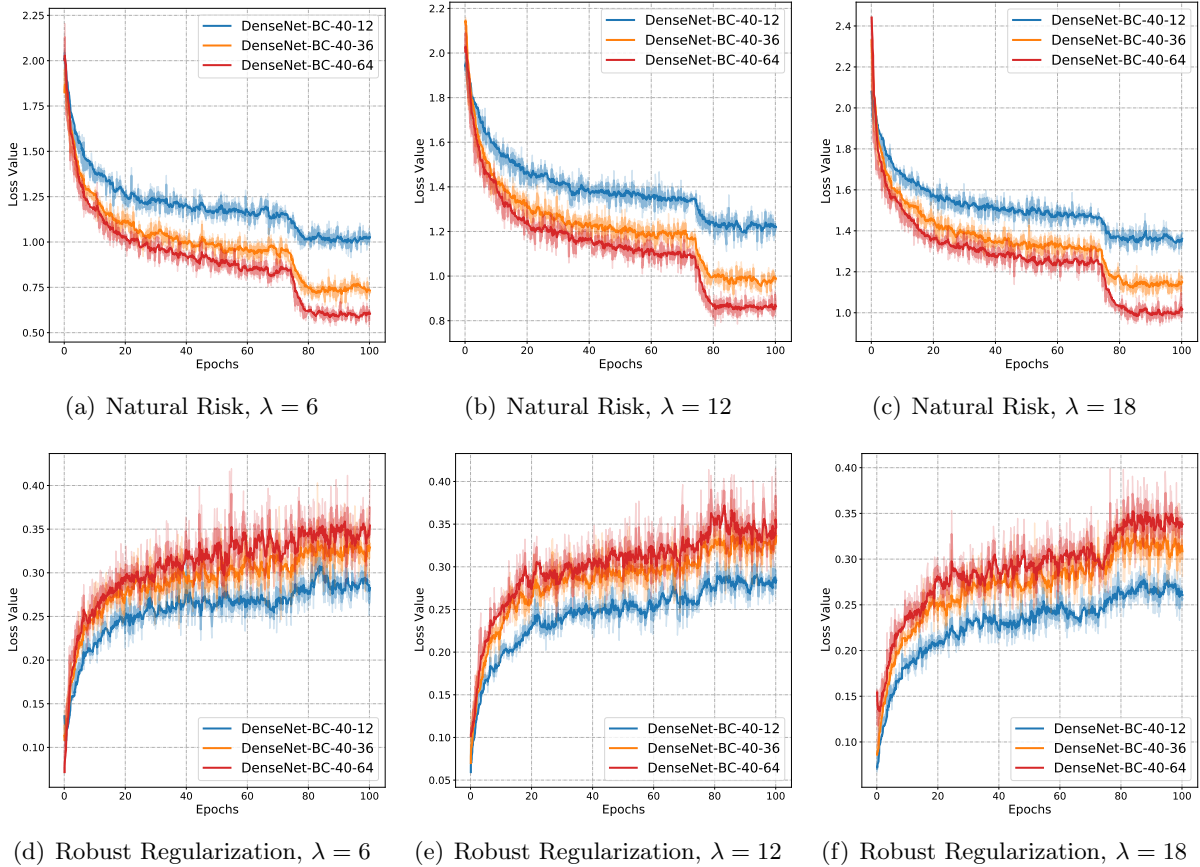


Figure 9: DenseNet-BC-40 on CIFAR10.

BUBECK, S., LI, Y. and NAGARAJ, D. (2020). A law of robustness for two-layers neural networks. *arXiv preprint arXiv:2009.14444* .

CAO, Y. and GU, Q. (2019). Generalization bounds of stochastic gradient descent for wide and deep neural networks. In *Advances in Neural Information Processing Systems*.

CARLINI, N. and WAGNER, D. A. (2017). Towards evaluating the robustness of neural networks. In *SP*. IEEE Computer Society.

CARMON, Y., RAGHUNATHAN, A., SCHMIDT, L., DUCHI, J. C. and LIANG, P. (2019). Unlabeled data improves adversarial robustness. In *NeurIPS*.

CHEN, J. and GU, Q. (2020). Rays: A ray searching method for hard-label adversarial attack. In *Proceedings of the 26th ACM SIGKDD International Conference on Knowledge Discovery and Data Mining*.

CHEN, J., ZHOU, D., YI, J. and GU, Q. (2020). A frank-wolfe framework for efficient and effective adversarial attacks. In *AAAI*.

- CHEN, P., ZHANG, H., SHARMA, Y., YI, J. and HSIEH, C. (2017). ZOO: zeroth order optimization based black-box attacks to deep neural networks without training substitute models. In *AISec@CCS*. ACM.
- CISSÉ, M., BOJANOWSKI, P., GRAVE, E., DAUPHIN, Y. N. and USUNIER, N. (2017). Parseval networks: Improving robustness to adversarial examples. In *ICML*, vol. 70 of *Proceedings of Machine Learning Research*. PMLR.
- COHEN, J. M., ROSENFELD, E. and KOLTER, J. Z. (2019). Certified adversarial robustness via randomized smoothing. In *ICML*, vol. 97 of *Proceedings of Machine Learning Research*. PMLR.
- CROCE, F. and HEIN, M. (2020a). Minimally distorted adversarial examples with a fast adaptive boundary attack. In *ICML*, vol. 119 of *Proceedings of Machine Learning Research*. PMLR.
- CROCE, F. and HEIN, M. (2020b). Reliable evaluation of adversarial robustness with an ensemble of diverse parameter-free attacks. In *ICML*.
- DHILLON, G. S., AZIZZADENESHELI, K., LIPTON, Z. C., BERNSTEIN, J., KOSSAIFI, J., KHANNA, A. and ANANDKUMAR, A. (2018). Stochastic activation pruning for robust adversarial defense. *ICLR*.
- DOBRIAN, E., HASSANI, H., HONG, D. and ROBEY, A. (2020). Provable tradeoffs in adversarially robust classification. *arXiv preprint arXiv:2006.05161*.
- FAWZI, A., FAWZI, O. and FROSSARD, P. (2018). Analysis of classifiers’ robustness to adversarial perturbations. *Mach. Learn.* **107** 481–508.
- GAO, R., CAI, T., LI, H., HSIEH, C.-J., WANG, L. and LEE, J. D. (2019). Convergence of adversarial training in overparametrized neural networks. In *Advances in Neural Information Processing Systems*.
- GILMER, J., METZ, L., FAGHRI, F., SCHOENHOLZ, S., RAGHU, M., WATTENBERG, M. and GOODFELLOW, I. (2018). Adversarial spheres.
- GOODFELLOW, I. J., SHLENS, J. and SZEGEDY, C. (2015). Explaining and harnessing adversarial examples. In *ICLR* (Y. Bengio and Y. LeCun, eds.).
- GOWAL, S., QIN, C., UESATO, J., MANN, T. and KOHLI, P. (2020). Uncovering the limits of adversarial training against norm-bounded adversarial examples. *arXiv preprint arXiv:2010.03593*.
- GU, S. and RIGAZIO, L. (2015). Towards deep neural network architectures robust to adversarial examples. In *ICLR* (Y. Bengio and Y. LeCun, eds.).
- GUO, C., RANA, M., CISSE, M. and VAN DER MAATEN, L. (2018). Countering adversarial images using input transformations. *ICLR*.
- HE, K., ZHANG, X., REN, S. and SUN, J. (2016a). Deep residual learning for image recognition. In *CVPR*.

- HE, K., ZHANG, X., REN, S. and SUN, J. (2016b). Identity mappings in deep residual networks. In *ECCV*.
- HEIN, M. and ANDRIUSHCHENKO, M. (2017). Formal guarantees on the robustness of a classifier against adversarial manipulation. In *Advances in Neural Information Processing Systems*.
- HENDRYCKS, D., LEE, K. and MAZEIKA, M. (2019). Using pre-training can improve model robustness and uncertainty. In *ICML*, vol. 97 of *Proceedings of Machine Learning Research*. PMLR.
- HUANG, G., LIU, Z., VAN DER MAATEN, L. and WEINBERGER, K. Q. (2017). Densely connected convolutional networks. In *2017 IEEE Conference on Computer Vision and Pattern Recognition*.
- ILYAS, A., ENGSTROM, L., ATHALYE, A., LIN, J., ATHALYE, A., ENGSTROM, L., ILYAS, A. and KWOK, K. (2018). Black-box adversarial attacks with limited queries and information. In *Proceedings of the 35th International Conference on Machine Learning*.
- ILYAS, A., ENGSTROM, L. and MADRY, A. (2019a). Prior convictions: Black-box adversarial attacks with bandits and priors. *ICLR* .
- ILYAS, A., SANTURKAR, S., TSIPRAS, D., ENGSTROM, L., TRAN, B. and MADRY, A. (2019b). Adversarial examples are not bugs, they are features. In *NeurIPS*.
- JACOBSEN, J., BEHRMANN, J., ZEMEL, R. S. and BETHGE, M. (2019). Excessive invariance causes adversarial vulnerability. In *ICLR*. OpenReview.net.
- JACOT, A., HONGLER, C. and GABRIEL, F. (2018). Neural tangent kernel: Convergence and generalization in neural networks. In *NeurIPS*.
- KRIZHEVSKY, A., HINTON, G. ET AL. (2009). Learning multiple layers of features from tiny images .
- KURAKIN, A., GOODFELLOW, I. J. and BENGIO, S. (2017). Adversarial machine learning at scale. In *ICLR*. OpenReview.net.
- LÉCUYER, M., ATLIDAKIS, V., GEAMBASU, R., HSU, D. and JANA, S. (2019). Certified robustness to adversarial examples with differential privacy. In *SP*. IEEE.
- LIAO, F., LIANG, M., DONG, Y., PANG, T., HU, X. and ZHU, J. (2018). Defense against adversarial attacks using high-level representation guided denoiser. In *CVPR*.
- MADRY, A., MAKELOV, A., SCHMIDT, L., TSIPRAS, D. and VLADU, A. (2018). Towards deep learning models resistant to adversarial attacks. In *ICLR*. OpenReview.net.
- MENG, D. and CHEN, H. (2017). Magnet: a two-pronged defense against adversarial examples. In *Proceedings of the 2017 ACM SIGSAC Conference on Computer and Communications Security*.
- MOOSAVI-DEZFOOLI, S., FAWZI, A. and FROSSARD, P. (2016). Deepfool: A simple and accurate method to fool deep neural networks. In *CVPR*. IEEE Computer Society.

- NAJAFI, A., MAEDA, S., KOYAMA, M. and MIYATO, T. (2019). Robustness to adversarial perturbations in learning from incomplete data. In *NeurIPS*.
- NAKKIRAN, P. (2019). Adversarial robustness may be at odds with simplicity. *CoRR abs/1901.00532*.
- PANG, T., YANG, X., DONG, Y., XU, K., SU, H. and ZHU, J. (2020). Boosting adversarial training with hypersphere embedding. *CoRR abs/2002.08619*.
- PAPERNOT, N., MCDANIEL, P. D., JHA, S., FREDRIKSON, M., CELIK, Z. B. and SWAMI, A. (2016a). The limitations of deep learning in adversarial settings. In *EuroS&P*. IEEE.
- PAPERNOT, N., MCDANIEL, P. D., WU, X., JHA, S. and SWAMI, A. (2016b). Distillation as a defense to adversarial perturbations against deep neural networks. In *SP*. IEEE Computer Society.
- PAULAVIČIUS, R. and ŽILINSKAS, J. (2006). Analysis of different norms and corresponding lipschitz constants for global optimization. *Technological and Economic Development of Economy* **12** 301–306.
- QIN, C., MARTENS, J., GOWAL, S., KRISHNAN, D., DVIJOTHAM, K., FAWZI, A., DE, S., STANFORTH, R. and KOHLI, P. (2019). Adversarial robustness through local linearization. In *NeurIPS*.
- RAGHUNATHAN, A., XIE, S. M., YANG, F., DUCHI, J. and LIANG, P. (2020). Understanding and mitigating the tradeoff between robustness and accuracy. *arXiv preprint arXiv:2002.10716* .
- RAGHUNATHAN, A., XIE, S. M., YANG, F., DUCHI, J. C. and LIANG, P. (2019). Adversarial training can hurt generalization. *CoRR abs/1906.06032*.
- RICE, L., WONG, E. and KOLTER, J. Z. (2020). Overfitting in adversarially robust deep learning. *CoRR abs/2002.11569*.
- SALMAN, H., LI, J., RAZENSHTEYN, I. P., ZHANG, P., ZHANG, H., BUBECK, S. and YANG, G. (2019). Provably robust deep learning via adversarially trained smoothed classifiers. In *NeurIPS*.
- SAMANGOUEI, P., KABKAB, M. and CHELLAPPA, R. (2018). Defense-gan: Protecting classifiers against adversarial attacks using generative models. *ICLR* .
- SCHMIDT, L., SANTURKAR, S., TSIPRAS, D., TALWAR, K. and MADRY, A. (2018). Adversarially robust generalization requires more data. In *NeurIPS*.
- SEHWAG, V., WANG, S., MITTAL, P. and JANA, S. (2020). On pruning adversarially robust neural networks. *CoRR abs/2002.10509*.
- SONG, Y., KIM, T., NOWOZIN, S., ERMON, S. and KUSHMAN, N. (2018). Pixeldefend: Leveraging generative models to understand and defend against adversarial examples. *ICLR* .

- SZEGEDY, C., ZAREMBA, W., SUTSKEVER, I., BRUNA, J., ERHAN, D., GOODFELLOW, I. J. and FERGUS, R. (2014). Intriguing properties of neural networks. In *ICLR* (Y. Bengio and Y. LeCun, eds.).
- TRAMÈR, F., PAPERNOT, N., GOODFELLOW, I. J., BONEH, D. and MCDANIEL, P. D. (2017). The space of transferable adversarial examples. *CoRR* **abs/1704.03453**.
- TSIPRAS, D., SANTURKAR, S., ENGSTROM, L., TURNER, A. and MADRY, A. (2019). Robustness may be at odds with accuracy. In *ICLR*. OpenReview.net.
- WANG, Y., MA, X., BAILEY, J., YI, J., ZHOU, B. and GU, Q. (2019). On the convergence and robustness of adversarial training. In *ICML*.
- WANG, Y., ZOU, D., YI, J., BAILEY, J., MA, X. and GU, Q. (2020). Improving adversarial robustness requires revisiting misclassified examples. In *ICLR*. OpenReview.net.
- WENG, T.-W., ZHANG, H., CHEN, P.-Y., YI, J., SU, D., GAO, Y., HSIEH, C.-J. and DANIEL, L. (2018). Evaluating the robustness of neural networks: An extreme value theory approach. In *International Conference on Learning Representations*.
- WONG, E., RICE, L. and KOLTER, J. Z. (2020). Fast is better than free: Revisiting adversarial training. *CoRR* **abs/2001.03994**.
- WU, D., XIA, S.-T. and WANG, Y. (2020). Adversarial weight perturbation helps robust generalization. *Advances in Neural Information Processing Systems* **33**.
- XIE, C., WANG, J., ZHANG, Z., REN, Z. and YUILLE, A. (2018). Mitigating adversarial effects through randomization. *ICLR* .
- YANG, Y.-Y., RASHTCHIAN, C., ZHANG, H., SALAKHUTDINOV, R. R. and CHAUDHURI, K. (2020). A closer look at accuracy vs. robustness. *Advances in Neural Information Processing Systems* **33**.
- ZAGORUYKO, S. and KOMODAKIS, N. (2016). Wide residual networks. In *BMVC*. BMVA Press.
- ZHANG, H., YU, Y., JIAO, J., XING, E. P., GHAOUI, L. E. and JORDAN, M. I. (2019). Theoretically principled trade-off between robustness and accuracy. In *ICML*, vol. 97 of *Proceedings of Machine Learning Research*. PMLR.
- ZHANG, J., XU, X., HAN, B., NIU, G., CUI, L., SUGIYAMA, M. and KANKANHALLI, M. S. (2020a). Attacks which do not kill training make adversarial learning stronger. *CoRR* **abs/2002.11242**.
- ZHANG, X., CHEN, J., GU, Q. and EVANS, D. (2020b). Understanding the intrinsic robustness of image distributions using conditional generative models. In *Proceedings of the 23rd International Conference on Artificial Intelligence and Statistics*.
- ZOU, D., CAO, Y., ZHOU, D. and GU, Q. (2020). Gradient descent optimizes over-parameterized deep relu networks. *Machine Learning* **109** 467–492.